Quasiparticle and Josephson tunneling of overdoped $Bi_2Sr_2CaCu_2O_{8+\delta}$ single crystals

Lutfi Ozyuzer
Science and Technology Center for Superconductivity and Materials Science Division, Argonne National Laboratory, Argonne, Illinois 60439;
Illinois Institute of Technology, Chicago, Illinois 60616;
and Department of Physics, Izmir Institute of Technology, TR-35230 Izmir, Turkey

John F. Zasadzinski
Science and Technology Center for Superconductivity and Materials Science Division, Argonne National Laboratory, Argonne, Illinois 60439
and Illinois Institute of Technology, Chicago, Illinois 60616

Chris Kendziora
Naval Research Laboratory, Washington, DC 20375

K. E. Gray
Science and Technology Center for Superconductivity and Materials Science Division, Argonne National Laboratory, Argonne, Illinois 60439

(Received 29 July 1998; revised manuscript received 18 October 1999)

The point contact tunneling technique is used to examine quasiparticle and Josephson currents in overdoped $Bi_2Sr_2CaCu_2O_{8+\delta}$ (Bi-2212) single crystals with bulk T_c values ranging from 82 K down to 62 K. Superconductor–insulator–normal-metal (SIN) tunnel junctions are formed between Bi-2212 crystals and a Au tip, which display well-resolved quasiparticle gap features including sharp conductance peaks. Reproducible superconductor-insulator-superconductor (SIS) tunnel junctions are also obtained between two pieces of the Bi-2212 crystals, resulting in simultaneous quasiparticle and Josephson currents. The dynamic conductances of both SIN and SIS junctions are qualitatively similar to those found on optimally doped Bi-2212, but with reduced gap values, e.g., $\Delta = 15-20$ meV for $T_c = 62$ K. Fits to the conductance data in the gap region are obtained using a model with $d_{x^2-y^2}$ symmetry, and it is shown that this provides a better fit than *s*-wave symmetry. Both SIN and SIS tunneling conductances also display dip and hump features at high bias voltages similar to those found on optimal and underdoped crystals, indicating that these are intrinsic properties of the quasiparticles. The SIS data indicate that these features appear to be part of a larger spectrum that extends out to 300–400 mV. The Josephson current has been measured for 13 SIS junctions on the 62 K crystals with resistances varying over two decades. It is found that the maximum value depends on junction resistance in a manner consistent with Ambegaokar-Baratoff theory, but with a reduced I_cR_n product.

I. INTRODUCTION

Most of the early studies on the high-T_c superconductors (HTS's) focused on the physical and chemical properties of optimally doped compounds where the critical temperature T_c is the highest value. Recently, the doping dependence of the HTS's has become a significant issue due to pseudogap phenomena in underdoped compounds and to the peculiar influence of hole concentration on superconducting properties such the energy gap[1] and spectral features of the tunneling density of states (DOS).[1,2] One question that arises is whether the pairing symmetry is affected by doping. The symmetry of the superconducting order parameter for the optimally doped HTS's is consistent with $d_{x^2-y^2}$(*d*-wave) as found in angle-resolved photoemission spectroscopy[3,4] (ARPES) experiments on $Bi_2Sr_2CaCu_2O_{8+\delta}$ (Bi-2212) and tricrystal ring[5,6] experiments on $YBa_2Cu_3O_{7-x}$ and $Tl_2Ba_2CuO_{6+\delta}$. The possibility of gap symmetry conversion from *d*-wave to *s*-wave with overdoping of Bi-2212 is suggested by Kendziora *et al.*[7] and Kelley *et al.*[8] using Raman and ARPES studies respectively. Tunneling measurements of the strong-coupling ratio $2\Delta/k_BT_c$ in Bi-2212 indicate a decrease from a value of 9.3 for optimally doped samples to values approaching the BCS mean-field value with overdoping.[1] This is consistent with the generally held view that overdoped cuprates, being farther away from antiferromagnetic insulating phase of the undoped compounds, may exhibit more conventional Fermi liquid behavior.

It thus has become clear that the overdoped region of HTS's is interesting in its own right, serving as a possible base line from which the stronger electron correlations found in underdoped materials might be understood. In this article we focus on tunneling spectroscopy measurements on overdoped crystals of Bi-2212. We find that the tunneling spectra are qualitatively similar to those found on optimally doped crystals, but with a reduced energy scale, i.e., typical Δ values are 15–20 meV for a crystal with $T_c = 62$ K, compared to 38 meV for optimal doping.[1,2,9,10] In general, the gap region spectra are consistent with *d*-wave symmetry and there is no evidence of a crossover to *s*-wave symmetry with overdop-

 ©2000 The American Physical Society

ing. We present a more detailed examination and discussion of the dip and hump spectral features found at high bias, suggesting that these a part of a larger spectrum that extends out to 300–400 mV. Finally, we present the results on the Josephson current measured in more than a dozen break junctions where it is concluded that coherent tunneling processes along the *c* axis are important in the superconducting state.

The optimally doped compound of Bi-2212 has a T_c onset of 95 K and its T_c can be reduced either by additional oxygen content (overdoping) or by the removal of oxygen with vacuum annealing (underdoping).[1,2,11] Thus Bi-2212 is a perfect candidate for studying its physical properties over a large range of the doping phase diagram. Furthermore, Bi-2212 can be grown as a single crystal with a very low defect density and a very flat surface after cleaving, making it suitable for surface sensitive experiments such as scanning tunneling microscopy (STM), Raman, and ARPES. Tunneling spectroscopy is one of the most powerful methods for studying the DOS near the Fermi level,[12,13] and the reliability of point contact tunneling (PCT) spectroscopy has been proven for conventional superconductors[14] such as Nb where strong-coupling phonon structures have been observed similar to those found in planar junctions. Tunneling studies of Bi-2212 by PCT (Refs. 1 and 2) and STM (Refs. 2, 9, 15, and 16) have shown that the spectra are very similar for these two techniques despite the fact that PCT has a larger junction area and relies on a surface tunnel barrier. Planar junctions on Bi-2212 have in general exhibited more broadened gap region conductances[17,18] compared to PCT or STM, but have better mechanical stability allowing easier temperature dependence measurements.

Near-optimally doped Bi-2212 has been examined by almost all of the available tunneling methods[12] including break junctions,[1,19,20] PCT,[1,2,21] and STM.[1,2,9,15,16,22] There is a wide scatter in the measured values of the superconducting gap parameter Δ. Reported values of Δ range from 20 to 50 meV.[12] Recent measurements by STM, PCT, and break junctions[1,2,9] on high-quality crystals show that this wide spread is likely due to the sensitive dependence of the superconducting gap on hole doping, which tends to exacerbate problems associated with inhomogeneous doping or surface effects. Because of a better understanding of HTS chemistry and fabrication, the quality of Bi-2212 crystals has improved considerably. Better control of the purity of the crystal narrows the spectrum of obtained energy gap values for a given doping level, and now it can be stated with some confidence that for optimally doped Bi-2212 with a T_c onset of 93–95 K, Δ is around 38 meV.[2,9,10] This improved reproducibility has allowed the observation by PCT and break junctions of a remarkable effect whereby the superconducting gap in Bi-2212 changes substantially and monotonically with doping over a narrow doping region where the T_c has a maximum.[1] On the overdoped side this effect has been seen by STM as well.[2,15,16,22]

The overdoped Bi-2212 single crystals examined here have T_c values of 82, 78, and 62 K, with the lowest T_c samples forming the bulk of this study. A few of the results have been published in Ref. 2 cited above, but here we present much more new data as well as a more detailed examination of the spectra. The tunneling spectra from both superconductor–insulator–normal-metal (SIN) and superconductor-insulator-superconductor (SIS) junctions exhibit the same qualitative features as found on optimally doped crystals, but with a reduced gap size. We discuss the extraction of the energy gap from SIN and SIS junctions using both *s*- and *d*-wave analyses. For the SIN data the gap region spectra are clearly more consistent with a *d*-wave DOS. The gap magnitudes are insensitive to the particular gap symmetry used for fitting, and there is good reproducibility. For example, we find that $\Delta = 15-20$ meV from more than 50 junctions (both SIN and SIS) on four different crystals with $T_c = 62$ K. Typical spectral features of SIN junctions include a weakly decreasing background conductance, asymmetric conductance peaks, and a dip and hump structure at high bias. The SIS junctions also exhibit the dip and hump structure as well as a higher-energy tail feature that extends out to 300–400 mV. All of these features are consistent with those found on optimally doped junctions,[1,2,9,19] and this gives further support to the idea that these are intrinsic quasiparticle features.

The SIS junctions, which we will argue are *c*-axis junctions, exhibit a simultaneous, well-defined quasiparticle gap and Josephson current when the junction conductance exceeds a critical value of about 10 μS. We find a correlation between the maximum Josephson current I_c and the normal-state junction resistance R_n, the latter value varying by nearly two decades. This establishes a basis for comparing the I_cR_n product to the measured quasiparticle gap. Our largest I_cR_n is about 7 meV, which is over 40% of the gap magnitude, a surprising result for *d*-wave superconductors, which indicates that the *c*-axis tunneling process is very coherent in the superconducting state. For two particular SIS junctions which exhibit clean quasiparticle conductances, a comparison is made between two model fits to the data: a smeared BCS DOS and a momentum-averaged *d*-wave DOS. We find that the *d*-wave fit is in better agreement with the subgap region, but that neither model adequately fits the data beyond 2Δ. The deviations for $eV > 2\Delta$ between the data and model fits are consistent among all of the junctions, and perhaps these features are signaling strong quasiparticle lifetime effects analogous to phonon structures observed in conventional superconductors.

II. EXPERIMENT

Samples of single-crystal Bi-2212 were grown by a self-flux technique in a strong thermal gradient to stabilize the direction of solidification. Extreme overdoping has been accomplished using stainless steel cells sealed with samples immersed in liquid oxygen, as described elsewhere.[11] Tunneling measurements were performed on four such crystals with T_c nearly 62 K, and a transition width of about 1 K. Magnetization measurements were taken after each tunneling measurement, and no significant change of T_c has been observed. Similarly prepared crystals annealed in flowing high oxygen pressure yielded T_c values of 78 K, and these were studied as well. For comparison, crystals grown by a floating zone process[1,2] were examined. These crystals had optimal T_c onsets of 95 K and using high-pressure oxygen annealing resulted in $T_c = 82$ K. The tunneling spectra obtained on the differently prepared crystals all displayed the same basic

characteristics. Tunneling measurements were done with the apparatuses[23] cooled by ^{4}He gas coupled to a liquid helium bath. Cleaved single-crystal samples of overdoped Bi-2212 usually have a shiny surface on the *a-b* plane. Each is mounted on a substrate using an epoxy so that the tip approaches along the *c* axis. Normally a Au tip was used as a counterelectrode, and it was mechanically and chemically cleaned before each run.

The SIN and SIS junctions are formed as follows. After the sample is placed in the measurement system and cooled down to 4.2 K, the distance and contact force between the tip and sample are adjusted using a differential micrometer. In the ordinary way, a tip pushes onto the surface of the crystal and a stable mechanical junction forms between the tip and crystal. Here the insulating tunnel barrier is the native surface layer of the crystal. The two neighboring Bi-O planes in Bi-2212 have weak bonds compared to Cu-O and Sr-O layers. Therefore the cleaved surface of Bi-2212 is a single Bi-O plane, and presumably the barrier is due to this layer and the underlying Sr-O layer. STM studies have indicated that this surface layer is semiconducting with an energy gap of at least 200 meV.[17] While the tip is pushed against the crystal, the *I-V* curve is continuously monitored on an oscilloscope until a suitable junction is obtained. Such junctions clearly display a superconducting gap in the *I-V* characteristics. The first derivative measurement $\sigma = dI/dV$ were obtained using a kelvin bridge circuit with the usual lock-in procedure. $I(V)$ and $dI/dV(V)$ were simultaneously plotted on a chart and recorded on computer. The junction resistances range from 300 Ω to 50 kΩ for the SIN junctions, but the majority of junctions fall in a narrower range ~2k–10kΩ. Although the tip approaches nominally along the *c* axis, the tunneling direction is not known with certainty, but we will argue later that both the SIN and SIS junctions have the tunnel barrier perpendicular to the *c* axis. The junction area is also not known with certainty; however, a good estimate for the SIN junctions is found from similar PCT measurements of Nb,[14] where the barrier height analysis of the tunneling conductance led to a contact diameter of ~2400 Å.

Increasing the force of the tip against the crystal produces an Ohmic contact (~1 Ω) between the tip and crystal, likely due to a perforation of the barrier layer. This results in a mechanical bond between Au and Bi-2212 because, when the tip is elevated, often a piece of Bi-2212 crystal also goes up that is fastened to the tip. We have found that it is not necessary to raise the tip to form a SIS junction, but merely to relieve the pressure. Presumably, in this case, one of the Bi-O plane pairs is separated and this results in an SIS junction, which forms between different parts of the crystal. The dislodged piece probably remains in the cavity in the larger crystal as these SIS junctions are mechanically very stable. As a consequence, this technique provides a fresh junction that is formed *in situ* deep in the crystal, thereby minimizing the exposure of the surface. A proposed schematic of the SIS junction between two pieces of crystal is represented in Fig. 1. The junction area is again uncertain; however, for a rough idea, the lateral size of a few attached crystallites was on the order of 100 μm on edge, so this provides an upper bound to the area. The thickness of the crystallites was much less than the lateral dimensions so that *c*-axis transport is generally favored. Our SIS conductance characteristics are very similar

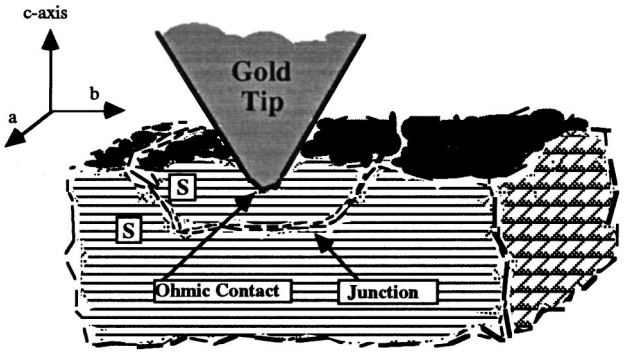

FIG. 1. Schematic representation of SIS junction formed by a Au tip.

to those of Yurgens *et al.*,[24] on intrinsic Bi-2212 *c*-axis junctions measured in small-area mesas intercalated with $HgBr_2$, which typically had a junction resistance per unit area of 0.5 $\Omega/\mu m^2$. Using this value and a typical junction resistance of 5 kΩ, we obtain an estimated junction area of 10^4 μm^2, consistent with our measured lateral area. We thus imagine that our break junctions consist of barriers where the adjacent Bi-O layers have been separated slightly by cleaving, similar to what happens when an intercalate is placed in between adjacent Bi-O layers. Based on the schematic of Fig. 1, it is not obvious why junctions between *a-b* planes do not contribute to the current, but as we will demonstrate, the conductance characteristics are not consistent with such junctions.

The SIN and SIS junctions were easily identified by their characteristic tunneling conductances. SIN junctions display an asymmetric, weakly decreasing background, an asymmetric dip and hump feature, and as low as 10%–15% zero-bias conductance. The SIS junctions have a symmetric background, less than 1% zero bias conductance, symmetric dip and hump features, and conductance peaks at 2Δ. In addition, the SIS junctions exhibit a hysteretic Josephson current when the junction resistance is below 100 kΩ.

III. RESULTS OF SIN JUNCTIONS

Before showing the experimental results, we review here the basic theoretical approach to analyzing the tunneling data. The tunneling current in an SIN junction can be written as[13]

$$I(V) = c \int |T|^2 N_{sn}(E) N_{nn}(E+eV)[f(E)-f(E+eV)]dE, \tag{1}$$

where $f(E)=[1+\exp(E/k_BT)]^{-1}$ is the Fermi function, $N_{sn}(E)$ is the DOS of the superconductor, $N_{nn}(E)$ is DOS of the normal metal which is Au in our case, $|T|^2$ is the tunneling matrix element, and *c* is a proportionality constant. The quasiparticle energy is given by *E*, which is defined relative to the Fermi level. For a rough estimation of the tunneling current, we consider $T=0$ K and assume that N_{nn} is a constant near the Fermi level and the tunneling matrix element $|T|^2$, has a weak energy dependence over the voltage range of the energy gap. Then,

$$dI/dV \equiv \sigma_s = c|T|^2 N_{sn}(E) = c|T|^2 N_s(E) N_n(E), \tag{2}$$

where we have now set $E=eV$. $N_s(E)$ is the superconducting part of the DOS, and $N_n(E)$ is the normal-state DOS of the superconductor. In most low-T_c superconductors, $N_n(E)$ usually is a constant over the energy range of interest. The ratio of σ_s/σ_n gives the superconducting DOS. According to BCS theory, the superconducting DOS is

$$N_s(E)=\mathrm{Re}\left\{\frac{E}{\sqrt{E^2-\Delta^2}}\right\}, \quad |E|\geqslant\Delta,$$

$$N_s(E)=0, \quad |E|<\Delta. \tag{3}$$

For conventional superconductors, the energy gap Δ is a constant in **k** space (isotropic *s*-wave pairing symmetry). However, for superconductors with *d*-wave pairing symmetry, the energy gap is anisotropic on the Fermi surface. In a two-dimensional superconductor, a simple *d*-wave DOS suggested by Won and Maki[25] is given by

$$N_s(E,\mathbf{k})=\mathrm{Re}\left\{\frac{E-i\Gamma}{\sqrt{(E-i\Gamma)^2-\Delta(\mathbf{k})^2}}\right\}, \tag{4}$$

where $\Delta(\mathbf{k})=\Delta\cos(2\theta)$ is the **k**-dependent energy gap and θ is the polar angle in **k** space. The total superconducting DOS $N_s(E)$ is found by an integral over the polar angle θ. Here E is replaced by E-$i\Gamma$, where Γ is a smearing parameter to account for the quasiparticle lifetime.[26] *Note that when a* Δ *value is given for a d-wave analysis it represents the maximum value in momentum space.*

Figure 2 shows the dynamic conductances of three SIN junctions at 4.2 K (dots) obtained from three different overdoped crystals with $T_c=62$, 78, and 82 K. Negative voltage corresponds to removal of electrons from the superconductor or occupied quasiparticle states in the DOS. Each junction displays sharp conductance peaks in the range 20–25 mV and a decreasing background conductance out to 200 mV. Each junction also displays a pronounced dip and hump for negative bias that is also seen in tunneling studies[1,2,15,16] of optimally doped Bi-2212 and is consistent with ARPES (Refs. 3 and 4) measurements of the spectral weight function along the $(\pi,0)$ momentum direction. This dip feature is located at approximately twice the voltage of the conductance peak and hence is scaling with the superconducting gap itself. A possible explanation for the origin of the dip feature in terms of strong coupling effects is given in Ref. 2, but here we simply note that it is observed in the most overdoped crystals studied to date. The zero-bias conductances vary from 20% to 40% of the estimated normal-state conductance, but in a few cases we have seen values as low as 10%–15% in overdoped crystals. By inspection, it is seen that the subgap shapes in Fig. 2 are not consistent with ordinary *s*-wave superconducting gaps, but rather they display a more cusp-like shape near zero bias which is more suggestive of *d*-wave symmetry.

Note that none of the SIN junctions of Fig. 2 display any zero-bias conductance peak (ZBCP) and this is typical of our PCT junctions.[1,2] Kashiwaya *et al.*[27] calculated the differential conductance between a normal metal and a *d*-wave superconductor junction within the framework of Blonder-Tinkham-Klapwijk (BTK) theory,[28] which includes tunneling and Andreev reflection. For interfaces perpendicular to the *a*-*b* plane, these junctions typically display pronounced ZBCP features and smeared-out quasiparticle gap features. The experiments of Covington *et al.*[29] verified the predictions of Kashiwaya *et al.* and demonstrated that such ZBCP anomalies are typical for *a*-*b* plane junctions. Since we never observe this feature, this indicates that our SIN junctions all have the barrier parallel to the Cu-O planes, as would result if it originates from the native Bi-O layer on the cleaved crystal surface. Such interfaces do not change the sign of the *d*-wave order parameter for electrons upon reflection and therefore do not give rise to the Andreev bound states responsible for the ZBCP.[27]

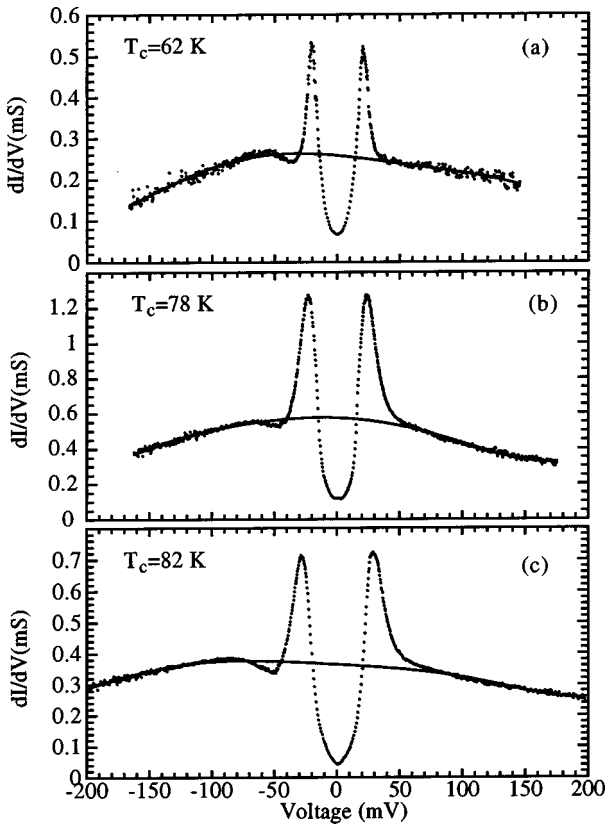

FIG. 2. Dynamic conductance of three SIN junctions (dots), from three different doping levels of overdoped Bi-2212 crystals at 4.2 K. The negative-bias region corresponds to occupied states in the DOS. The solid lines are estimated normal-state conductances (σ_N^*), which are generated from verifying the sum rule of the DOS.

Because of large upper critical fields[30] of HTSs, normal-state conductance cannot be obtained experimentally and it has to be estimated. Since the superconducting and normal-state conductances are expected to merge at voltages much higher than the gap, we can extrapolate the values of σ_s at high voltages and get an approximation σ_n^*, thus obtaining an approximate DOS from the ratio of σ_s/σ_n^*. We masked the superconducting gap region conductance out to the dip location, used a simple polynomial fit to obtain σ_n^*, and checked the resulting normalized conductance to make sure that the sum rule of the DOS, was verified. The solid lines in Fig. 2 represent estimated normal-state conductance curve using this procedure with a sixth-order polynomial. The inferred normal-state conductance, which exhibits a broad peak near bias, may be due to the underlying electronic structure of the Cu-O plane, which according to band structure calcu-

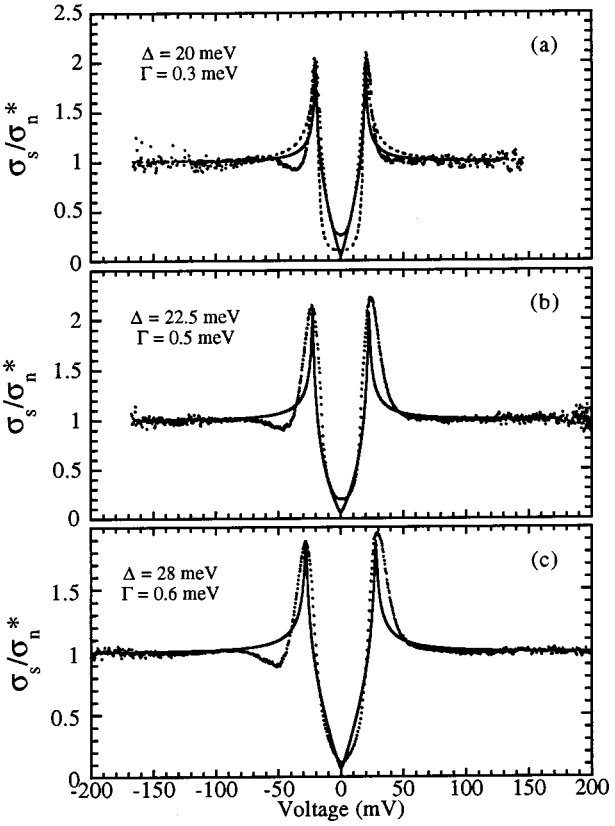

FIG. 3. Normalized conductance of three SIN junctions (dots), which are given in Fig. 2. The solid lines are *d*-wave fits which include the smearing factor Γ. Δ and Γ values are given in the figure for each fit. The dashed line in (a) is the smeared BCS DOS with $\Delta = 20$ meV and $\Gamma = 2$ meV.

lations and ARPES measurements[3,4] has a van Hove singularity near the Fermi energy which may be influencing the tunneling background.[31] Such a peak in the band structure DOS is a natural explanation for the consistent observation of the decreasing background in both PCT and STM.[2,9]

When the superconducting dynamic conductance is divided by σ_n^*, we obtain the normalized conductances (dots in Fig. 3), which can then be compared to a theoretical DOS to find the energy gap of the superconductor. The solid lines of Fig. 3 correspond to *d*-wave fits, and the parameters Δ and Γ are indicated on each plot. No least-squares fitting procedure was used; rather, the parameters were adjusted to best match the subgap region of the spectrum. The dashed line in Fig. 3(a) shows a fit from Eq. (1) using a smeared BCS DOS, i.e., Eq. (3), with the inclusion of a quasiparticle lifetime term Γ. The smeared BCS fit leads to an identical gap value, but a clearly much poorer fit to the subgap region of the conductance. This was found in all of the overdoped SIN junctions where the peak height to background PHB ratio was close to 2. Obviously, there is some uncertainty in σ_n^* near zero bias, but when we change the amount of data that are masked or the order of the polynomial fit, there is no change in the fitted gap value or in the comparison of *d*-wave vs. *s*-wave fits. In general, the *d*-wave fit was always better in the subgap region. Energy gaps vary from 15 to 20 meV for the SIN junctions on the 62 K samples, which leads to $2\Delta/k_BT_c$ in the range of 5.6–7.5. For optimally doped samples,[1,2,9,10] the corresponding $2\Delta/k_BT_c \sim 9.3$. This is very large when compared to a BCS ratio of 4.28 for a *d*-wave superconductor.[25] Thus we find that the energy gap decreases rapidly when T_c goes from 95 to 62 K, and the trend is to approach the BCS mean-field gap value. This rapid decrease of the gap with increased hole doping is also seen in ARPES experiments[32] and STM measurements[2,16] on overdoped Bi-2212.

The curves of Fig. 3 show that for $eV > \Delta$ the data do not match either the *d*-wave or *s*-wave models. This is not too surprising as these are BCS-type DOS which do not capture strong-coupling effects such as the quasiparticle decay processes found near peaks in the phonon density of states in conventional superconductors.[13] The dip and hump features may be indications of such quasiparticle decay processes as is suggested in ARPES.[3,4]

IV. RESULTS OF SIS JUNCTIONS

If both electrodes are identical superconductors in Eq. (1), the quasiparticle conductance peaks are at $\pm 2\Delta$. As a result of the convolution of the superconducting DOS, the quasiparticle peaks are sharper and zero-bias conductances are lower than SIN junctions. The Fermi function effect is very small compared to SIN junctions. In addition, Cooper pairs may tunnel through the barrier and a Josephson current occurs at zero bias in the *I-V* characteristics.[33]

In this part of the paper, highly reproducible and stable SIS junctions will be examined. Figures 4(a), 4(b), and 4(c) show current-voltage characteristics of three junctions from three different crystals with $T_c = 62$ K. These were measured at 4.2 K, and the junctions indicate SIS type, with very low leakage currents and sharp current onsets at $eV \sim 40$ meV, which is twice the gap value found in the SIN junctions. They also exhibit a hysteretic Josephson current at zero bias. Figure 4(d) shows the subgap region of Fig. 4(c) on a more sensitive scale to clearly show the hysteretic nature of the Josephson current. Hysteresis is a signature of Josephson junctions and is due to the fact that the current is switching from pair tunneling to single electron tunneling.

Figure 5 shows conductance-voltage characteristics of SIS junctions from three different 62 K samples at 4.2 K. The junction resistances are in the range 5–15 kΩ. Here the nearly vertical rise of the Josephson current produces a very large conductance peak at zero bias, which is off the scale. This is another clue that these zero-bias peaks are not the same as the ZBCP observed in *a-b* plane junctions.[27,29] Such Andreev bound states are part of the single-particle DOS, and when the spectral weight is shifted to the ZBCP it occurs at the expense of the superconducting gap features which are then heavily smeared out. As is seen in Fig. 5, the gap peaks are very sharp with large PHB ratios, which would not be consistent with the enormous peak at zero bias if it were due to Andreev bound states. The similarity of the quasiparticle spectra to intrinsic junctions of Yurgens *et al.*[24] indicates that these SIS break junctions are again *c* axis, which then provides an explanation for the absence of Andreev bound states.

The strong conductance peaks in Fig. 5 correspond to $\pm 2\Delta$ values. Symmetric dips are found near 3Δ as found on Bi-2212 crystals near optimal doping.[1,33] On average, the dip strength is low with respect to optimally doped samples.[1,2]

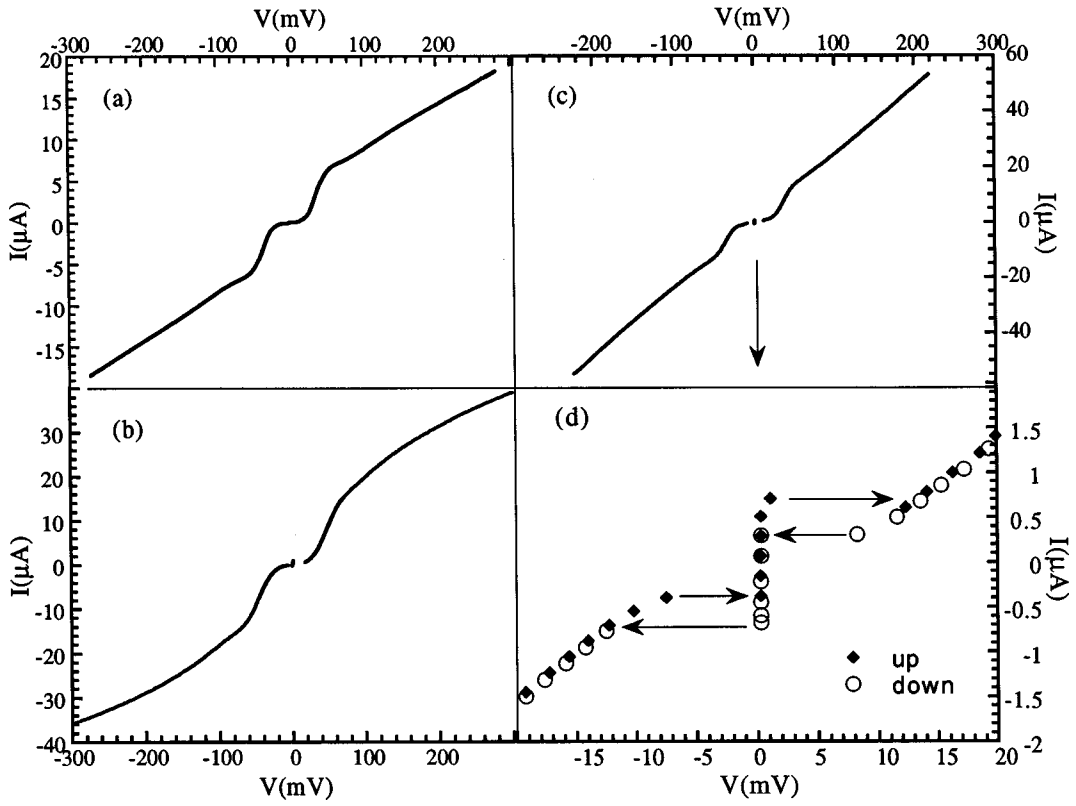

FIG. 4. The current-voltage characteristics of three different SIS junctions. (d) is an expanded scale of (c) near-zero bias for clarity. (d) shows hysteretic zero-bias feature which indicates a Josephson current.

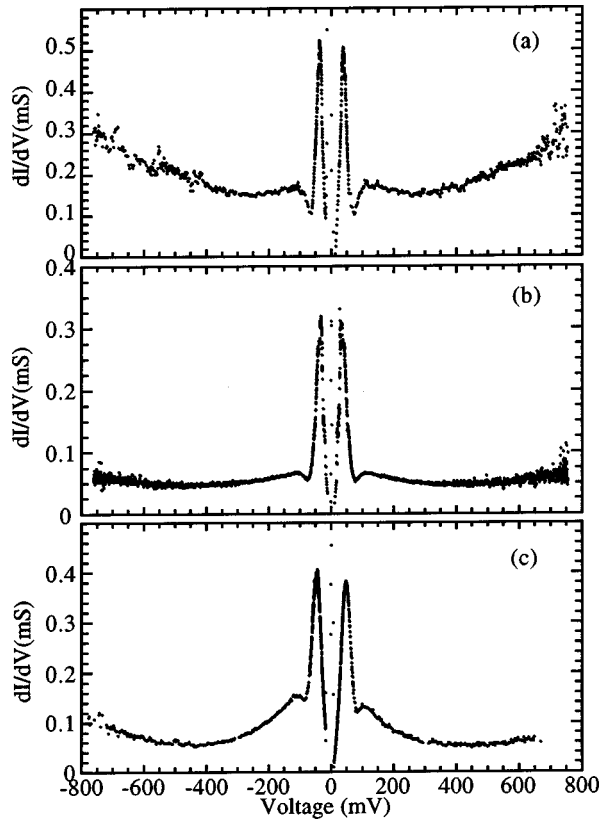

FIG. 5. The tunneling conductance of SIS junctions for overdoped Bi-2212. The upturn around ±300–400 mV may indicate that the bias is approaching the barrier height. The subgap tunneling conductance cannot be seen, because of switching.

The conductance at higher bias voltages ($e|V|>3\Delta$) at first decreases with increasing bias, as found in the SIN junctions. This behavior exists out to $|V|\sim 300$ mV, but for bias voltages beyond this value, there is an upturn in the conductance. A similar upturn is also observed in break junctions of Bi-2212 by Mandrus *et al.*[19] In the simple approximation expressed in Eq. (2), it is assumed that the tunneling matrix element $|T|^2$ is energy independent. However, at very high bias voltages we are likely approaching the barrier height potential. As a consequence of this, the tunneling transmission probability is increasing and the barrier height effect which gives a parabolic increase in conductance[13] may become dominant beyond ±300 mV.

The fact that the upturn in conductance occurs at nearly the same bias value in these junctions as well as other break junctions[19] which can differ in resistance by two orders of magnitude strongly argues against extrinsic effects such as heating as the cause of the initial decreasing background between 100 and 300 mV. Rather, the data suggest that the dip and hump feature is part of a larger spectrum that includes a tail extending out to 300–400 mV and that all of these features are intrinsic effects of the quasiparticle DOS in Bi-2212. These high-bias features are also consistent with what is found on the SIN junctions. It should be noted that a similar dip-hump-tail feature is found in the quasiparticle spectral weight function $A(\mathbf{k},\omega)$ measured in ARPES.[34] Although no definitive explanation of these spectral features exists, it is important to note the consistency between tunneling and ARPES.

In our preliminary analysis of these SIS data, the goal was to obtain the energy gap of the Bi-2212, and we used the simplest approach, which was to use Eq. (1) with a smeared

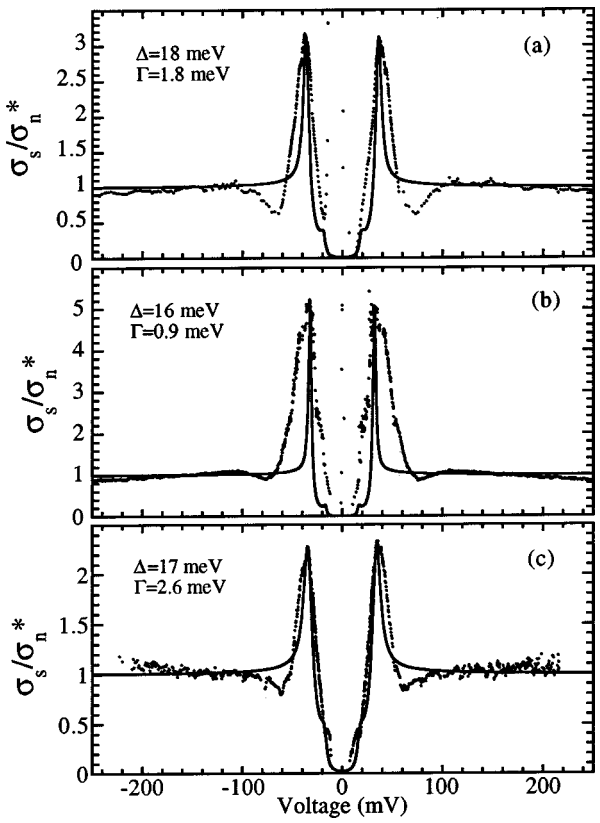

FIG. 6. The normalized tunneling conductance of SIS junctions (dots). (a) and (b) are the same data with Figs. 5(a) and 5(b). (c) is a different junction. The normalizations are conducted by a constant value which are chosen at 150 mV. The solid lines are BCS fits, which are calculated using given Δ and Γ values at graph and $T=4.2$ K.

BCS DOS for both electrodes. Furthermore, one of the key differences between *s*- and *d*-wave models of the SIS conductance is in the shape of the subgap region, which is difficult to obtain experimentally because of the switching property of the Josephson current. Thus a detailed comparison of the two models for every junction is not fruitful, and we found that an accurate estimate of 2Δ could be obtained directly from the conductance peak voltage. To demonstrate this, the data of Figs. 5(a) and 5(b) were normalized by a constant value which is the conductance at 150 mV. The normalized conductances are displayed in dots in Figs. 6(a) and 6(b). The steeper background shape in Fig. 5(c) did not allow us to normalize it with constant value, so we chose another junction (which was not measured to a high bias voltage) for normalization in Fig. 6(c). The solid lines in Fig. 6 represents SIS fits with the smeared BCS DOS and $T=4.2$ K. The Δ and Γ values are shown for each curve. Note that in each case the conductance peak voltage is exactly $2\Delta/e$. The quality of the fits in the subgap region varies, but the significance of this is difficult to assess since switching of the Josephson current can introduce structural artifacts near zero bias. The principal result here is that the energy gap values ($\Delta=16-18$ meV) are consistent with those found in SIN junctions. Considering all of the SIS junctions (>20) on the four different $T_c=62$ K crystals, the full range of gap values was $\Delta=15-20$ meV.

Up to now, we have shown the same gap value is obtained

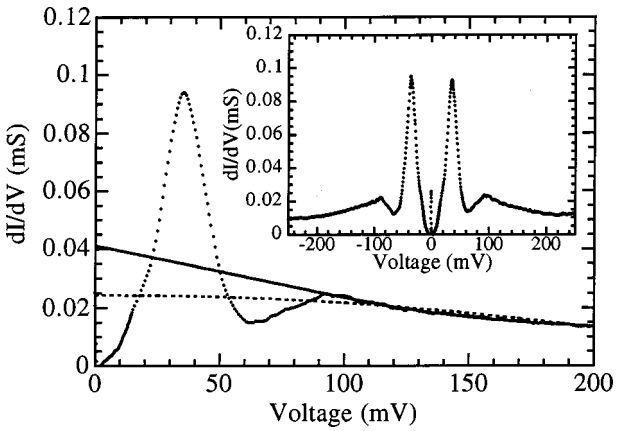

FIG. 7. The positive bias part of the tunneling conductance of SIS junctions (dots). Relatively small Josephson current helped to reveal subgap conductance very clearly. The solid line and dashed lines are two different estimated normal-state conductances. The inset shows the full spectrum.

from SIN data using either a *d*- or *s*-wave analysis, but that the *d*-wave fits were much better in the subgap region. The energy gaps inferred from the SIS data were consistent and found to be dramatically smaller than that of optimally doped Bi-2212. However, it is clear from the fits in Figs. 3(a) and 6 that a smeared BCS DOS does not adequately fit the data in the important subgap region. We now focus on a similar *d*-wave analysis of the quasiparticle conductance in SIS junctions. To do this we must choose relatively high-resistance junctions where the effects of the Josephson current are minimized. The inset of Fig. 7 shows another SIS tunneling conductance which is particularly clean. The Josephson current was very low for this particular junction due to its higher resistance (~ 40 kΩ) and a relatively small zero-bias conductance peak is observed. To obtain the subgap conductance very clearly, the dc bias current was swept very slowly inside the gap in both directions. These data also display generic Bi-2212 quasiparticle tunneling conductance characteristics such as sharp quasiparticle peaks and a dip and hump feature at high bias. Because the data are symmetric with bias polarity, we focus only on the positive-bias side of the spectrum. Our goal is to examine to what extent the shape of the subgap conductance in a SIS junction reveals information on pairing symmetry. Thus we consider the simple *d*-wave model of Eq. (4) for comparison to the smeared BCS model.

The data in Fig. 7 exhibit a strong decreasing background conductance at high bias which is consistent with the SIN data of Fig. 2, again indicating it is an intrinsic effect of the quasiparticle spectrum. But this background presents ambiguities in the normalization procedure. Therefore, we have used two different estimated normal-state conductances for the data which are shown in Fig. 7. For the first σ_n^*, we mask the data below 100 meV and extrapolate the background to Fermi level at zero bias (solid line in Fig. 7). For the second one, we obtain σ_n^* without masking any energy range in the spectra (dashed line in Fig. 7) and fitting with a third-order polynomial curve. This gives a higher PHB ratio than first one. The dots in Fig. 8(a) show the normalized tunneling conductance curve obtained from Fig. 7 using the dashed line normal state. The solid line in Fig. 8(a) is the smeared BCS fit, which is obtained from Eq. (1) with

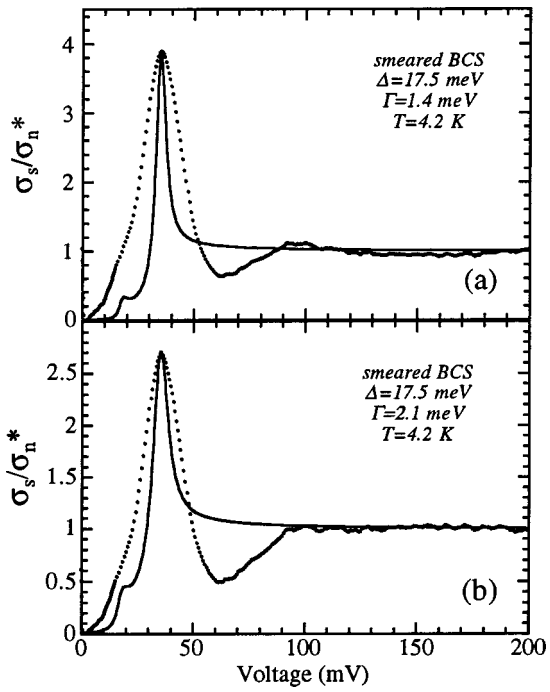

FIG. 8. The normalized conductances (dots) of the junction which is shown in Fig. 7. (a) Normalized by dashed line. (b) Normalized by solid line. The solid lines are SIS fits for BCS superconductors which are calculated for (a) $\Delta = 17.5\,\mathrm{meV}$, $\Gamma = 1.4\,\mathrm{meV}$, and $T = 4.2\,\mathrm{K}$, (b) $\Delta = 17.5\,\mathrm{meV}$, $\Gamma = 2.1\,\mathrm{meV}$, and $T = 4.2\,\mathrm{K}$.

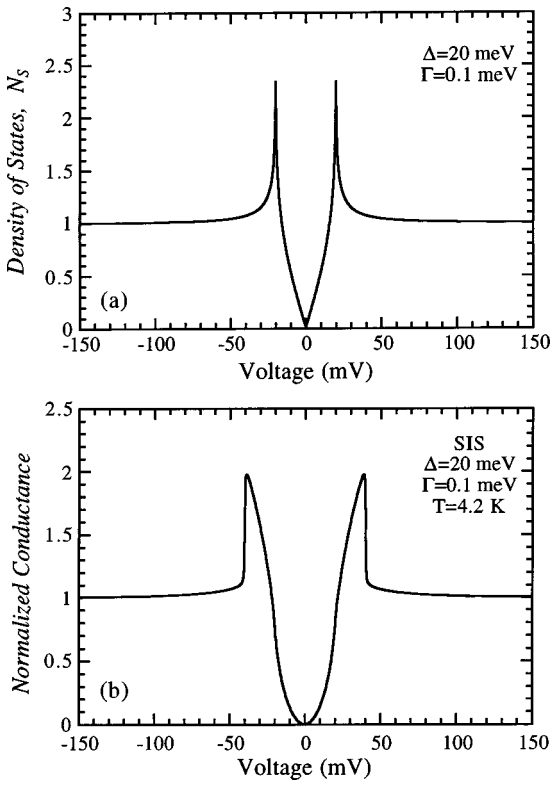

FIG. 9. The momentum-averaged DOS for a superconductor with $d_{x^2-y^2}$ pairing symmetry (a). The convolution of (a) with itself produces a SIS tunneling conductance (b).

$T = 4.2$ K to obtain the SIS tunneling conductance. The dots in Fig. 8(b) also show the normalized tunneling conductance curve obtained from Fig. 7 using the solid line normal state. Both fits reveal the value of $2\Delta = 35\,\mathrm{meV}$ which is consistent with the other junctions and as noted above could have been obtained directly from the conductance peak voltage. The overall quality of the fits is poor. The smaller subgap peak in the BCS fit near Δ arises from the Γ parameter while the data do not show such a distinct feature. This kink is not experimentally observed in any of the conventional or HTS SIS junctions to our knowledge. The broadening factor Γ is reasonably consistent with that obtained in similar fits to the SIN data.

Before discussing the *d*-wave fit of the SIS data, it is useful to present the generic features of the simplest model since these reveal some rather unique effects. Figure 9(a) shows a generated DOS curve for *d*-wave symmetry using Eq. (4). The underlying assumptions are that the Fermi surface is isotropic and the probability of tunneling is same for all **k** directions.[25] The cusp feature at zero bias is the basic indication of *d*-wave pairing symmetry. The SIS tunneling conductance curve is obtained with convolution of Fig. 9(a) with itself using Eq. (1), with $T = 4.2\,\mathrm{K}$, and this is shown in Fig. 9(b). Note that the maximum PHB ratio is ~ 2 for the model *d*-wave SIS tunneling conductance, whereas the normalized SIS curves of Figs. 6 and 8 suggest a PHB ratio that is much higher than 2. Thus we see at the outset that this simple *d*-wave model will not fit our data. One possible consideration is that our estimated normal-state curve is incorrect. While this cannot be ruled out, it is difficult to conceive of a normal-state conductance that would bring the PHB ratio from a value of 4 or 5 down to a value of 2 as the *d*-wave model requires.

Another possibility is that one or more of the underlying assumptions of the simple model are incorrect. ARPES results reveal that Bi-2212 has arch like Fermi surfaces in the four corners of the Brillouin zone[3,4] and this suggests the possibility that particular regions of momentum space are more heavily weighted than others in the contribution to the tunneling current, either due directly to the band structure or to the tunneling matrix element. These effects might be stronger in *c*-axis SIS junctions where identical Cu-O planes lie on either side of the barrier. For this reason we include a weighting function $f(\theta)$, to Eq. (4) as is in Refs. 35 and 36:

$$N_s(E,\theta) = f(\theta)\,\mathrm{Re}\left\{\frac{E - i\Gamma}{\sqrt{(E - i\Gamma)^2 - \Delta(\theta)^2}}\right\}, \qquad (5)$$

where $f(\theta) = 1 + \alpha\cos(4\theta)$ and the angle θ is measured with respect to the $(\pi,0)$ direction in the Brillouin zone. Here α is a directionality strength and the full quasiparticle DOS is obtained by integrating over θ. It should be emphasized that Eq. (5) is a phenomenological expression and there is no rigorous derivation of this result, but it can be seen immediately that this weighting function will qualitatively reproduce some of the conductance features observed in the experiment. Physically, the weighting function selects particular regions of the Brillouin zone, thereby minimizing the effects of gap anisotropy. For the extreme case of very strong directionality, a nearly constant gap would be obtained as is found

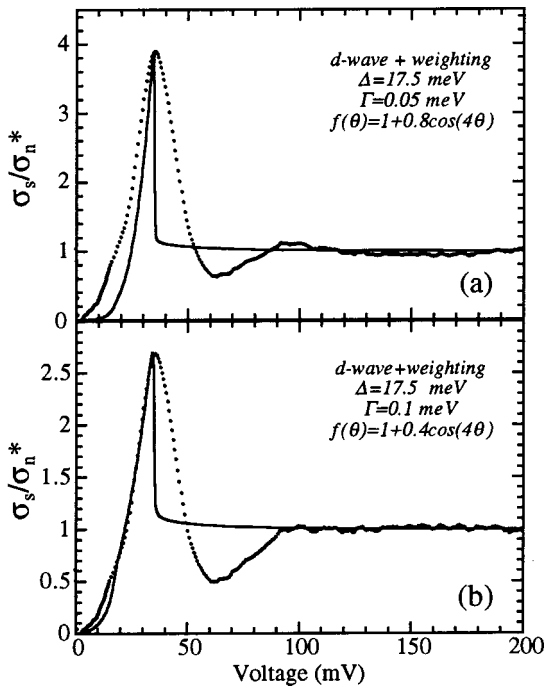

FIG. 10. The normalized conductance (dots) of the junction which is shown in Fig. 7. (a) The solid line is a SIS fit for a *d*-wave superconductor with weighting, $f(\theta)=1+0.8\cos(4\theta)$, which is calculated for $\Delta=17.5$ meV, $\Gamma=0.05$ meV, and $T=4.2$ K. (b) The parameters are $f(\theta)=1+0.4\cos(4\theta)$, $\Delta=17.5$ meV, $\Gamma=0.1$ meV, and $T=4.2$ K.

with *s*-wave symmetry and it has already been demonstrated that a smeared BCS DOS can exhibit a large PHB as shown in Fig. 8.

We fit the normalized SIS tunneling conductance, given in Figs. 8(a) and 8(b), using Eq. (5), and the solid lines in Figs. 10(a) and 10(b) show the resulting curve with $\Delta=17.5$ meV, $\Gamma=0.05$, $\alpha=0.8$ and $\Delta=17.5$ meV, $\Gamma=0.1$, $\alpha=0.4$, respectively. As before, note here that Δ is the maximum of $\Delta(\mathbf{k})$ and is the same magnitude as obtained with the BCS fit. For $eV<2\Delta$, the experimental results and fit are in better agreement than for the BCS fit in Fig. 8. As with the SIN junctions, the parameters have been adjusted to best match the subgap region. For $eV>2\Delta$ the fit shows an abrupt drop from the peak to background that is not found in the data. This feature appears to be generic to *d*-wave models [see Fig. 9(b)], but we have never observed it in over 50 SIS junctions on Bi-2212 with various hole doping[1,2] and to our knowledge such an abrupt drop has never been seen in the literature. Rather the experimental data invariably exhibit a much broader conductance peak followed by the dip and hump feature, which is also not found in this simple *d*-wave model. The inset of Fig. 11 shows another SIS junction which was chosen for analysis because of the relatively low Josephson current and clean quasiparticle data. This junction exhibits a smaller PHB ratio than in Fig. 10. The solid line in the Fig. 11 is the estimated normal-state conductance using second order polynomial fit. The normalized data are displayed in Fig. 12 along with the *d*-wave (solid line) and smeared BCS (dashed line) fit obtained with $\Delta=19.5$ meV, $\Gamma=1.5$, $\alpha=0.6$ and $\Delta=18.5$ meV, $\Gamma=3.5$, respectively. The larger Γ value reflects the generally broader features of this junction's spectrum, and there is better agreement with data in the subgap region. Nevertheless, for $eV>2\Delta$ the data display the same deviation from the fit as found in Fig. 10. Looking back to the *d*-wave fits in Fig. 3 for SIN data, there is a similar discrepancy for $eV>\Delta$. This suggests the possibility that these characteristics of the SIS spectra for $eV>2\Delta$ are intrinsic and not due to a less interesting effects such as a distribution of gap values due to sample inhomogeneity. It was recently argued that the dip feature is a strong-coupling effect[2] analogous to the phonon structures observed in conventional strong-coupled superconductors.[13] Perhaps the entire spectrum beyond 2Δ requires a full microscopic *d*-wave model, analogous to strong-coupling theory for conventional superconductors.

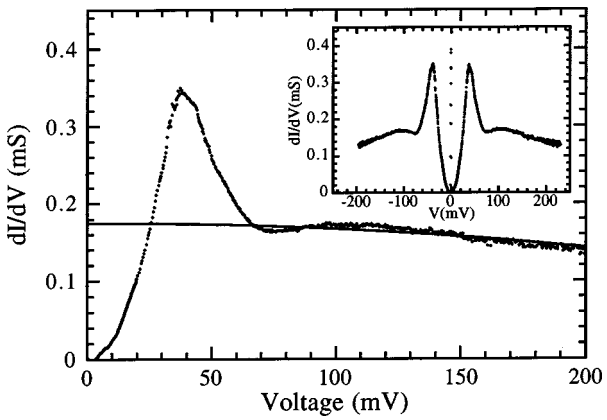

FIG. 11. The positive-bias part of the tunneling conductance of another SIS junction (dots). The solid line is an estimated normal-state conductance. The inset shows the full spectrum.

V. JOSEPHSON CURRENTS

In this part of the paper, we will present and discuss Josephson currents on overdoped Bi-2212. Reproducible Josephson tunnel junctions have been obtained, indicating both quasiparticle and Josephson tunneling currents simultaneously as we displayed in Fig. 4. Josephson currents are

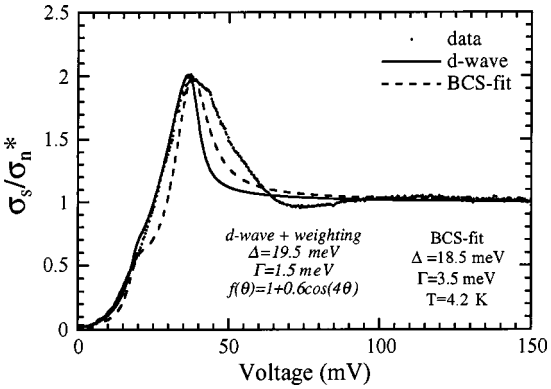

FIG. 12. The normalized conductance (dots) of the junction which is shown in Fig. 11. The solid line is a SIS fit for a *d*-wave superconductor with weighting, $f(\theta)=1+0.6\cos(4\theta)$, which is calculated for $\Delta=19.5$ meV, $\Gamma=1.5$ meV, and $T=4.2$ K. The dashed line is a SIS fit for BCS superconductors, which is calculated for $\Delta=18.5$ meV, $\Gamma=3.5$ meV, and $T=4.2$ K.

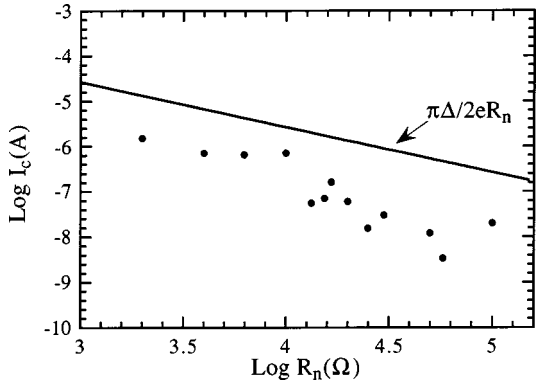

FIG. 13. Josephson current vs junction resistance for overdoped Bi-2212 at 4.2 K (dots) in logarithmic scale. The solid line is the Ambegaokar-Baratoff prediction for $\Delta = 17$ meV.

observed at 4.2 K when the junction conductance exceeds a minimum value. For the overdoped crystals here the minimum value was about 10 μS, whereas it was about 5 μS for near-optimal-doped Bi-2212 (Ref. 33). The hysteretic nature of the Josephson current is shown in Fig. 4(d), and the I_cR_n product for this particular junction is 3 mV. The Ambegaokar-Baratoff (AB) theory[37] for BCS superconductors predicts the relation

$$I_cR_n = \frac{\pi\Delta(0)}{2e}, \tag{6}$$

where I_c is the Josephson current, R_n is the resistance of the junction, and $\Delta(0)$ is the energy gap at 0 K. Figure 13 shows the measured critical current I_c as function of the junction resistance R_n for 13 different SIS junctions formed on the four overdoped ($T_c = 62$ K) Bi-2212 crystals. Note that the junction resistance varies by about two decades. The solid line corresponds to the maximum theoretical value expected from AB theory using $\Delta = 17$ meV, the average gap found in the quasiparticle data. The data show that the maximum Josephson current depends on junction resistance in a manner which is consistent with AB theory, but with a value of I_cR_n that is reduced from that expected using the average quasiparticle gap. This dependence of I_c vs R_n is important for it suggests that many of the underlying assumptions in AB theory can be carried over to the *d*-wave case. Furthermore, it all but rules out any possibility that the ZBCP anomalies are responsible[27] as these effects would not exhibit any correlation with R_n. We obtained a maximum of 7 mV for I_cR_n product [see Fig. 4(b)], which is approximately 40% of the expected magnitude, and the overall average is 2.4 mV.

While the average I_cR_n product is small compared to AB theory, it should be remembered that this theory applies to *s*-wave superconductors and assumes that the tunneling matrix element $T_{\mathbf{k},\mathbf{k}'}$ is a constant, independent of electron momentum. When this type of incoherent tunneling matrix element is applied to *d*-wave superconductors, one obtains $I_cR_n = 0$ to leading order.[38,39] This is a consequence of the changes in sign of the *d*-wave order parameter as one sums over momentum. Thus the I_cR_n products observed here are actually quite large for *d*-wave superconductors. The reason for these large values is probably an indication that there is a significant coherent part to the tunneling matrix element;[39] that is, $\mathbf{k}$ must equal $\mathbf{k}'$ for quasiparticle states on either side of the junction. In this case the signs of the order parameters are multiplied, i.e., $(+1)^2$ or $(-1)^2$, and this leads to a nonzero Josephson current for *d*-wave superconductors. It should be noted that recent measurements of the Josephson current for intrinsic *c*-axis junctions in Bi-2212 mesas[40] are also consistent with *d*-wave gap symmetry and coherent tunneling processes. This is a remarkable effect. Above T_c, the electronic system is generally not described by Fermi liquid theory and the *c*-axis transport is best understood by incoherent tunneling between Cu-O planes. However, in the superconducting state a simple *d*-wave gap is found that is consistent with a Fermi liquid ground state and the *c*-axis tunneling becomes coherent. Clearly, more experimental and theoretical work is needed to understand the magnitude of the Josephson I_cR_n products observed here and the nature of the *c*-axis tunneling process.

VI. SUMMARY AND CONCLUSION

We have performed PCT measurements on overdoped Bi-2212 single crystals with bulk T_c values near 62, 78, and 82 K. High quality reproducible SIN and SIS junctions were obtained, and the two junction types gave consistent results for the gap magnitudes as well as the high-bias spectra. The SIN data were clearly better fit in the subgap region to a simple *d*-wave DOS, indicating no evidence for any crossover to *s*-wave symmetry with overdoping. Attempts to fit the SIS spectra required a weighted, momentum-averaged *d*-wave DOS, and this might have significance for the tunneling processes in intrinsic *c*-axis junctions of single-crystal Bi-2212, implying that quasiparticles near the $(\pi,0)$ point tunnel more easily than those along the (π,π) direction. The *d*-wave fit led to identical gap values as found with a smeared BCS DOS, but with a somewhat improved fit to the subgap region of the conductance. The measured gaps on the overdoped crystals are reduced considerably from that found on optimally doped crystals. The value of the strong-coupling parameter $2\Delta/kT_c$ is between 5.6 and 7.5, reduced from the value of 9.3 found on optimally doped samples, and this indicates a trend toward weak-coupling, mean-field behavior as hole doping is increased.

The dynamic conductance spectra of the SIN and SIS junctions are qualitatively similar to those found on optimally doped[1,2,9,10] and near-optimally doped crystals[16] with all junctions exhibiting *d*-wave-like subgap conductance, sharp conductance peaks, and a dip-hump-tail feature that is also seen in the quasiparticle spectral weight measured by ARPES.[34] The position of the dip is $\sim 2\Delta$ for SIN junctions and $\sim 3\Delta$ for SIS junctions. Thus the energy scale for the dip feature is set by the superconducting gap value. This strongly suggests that the dip-hump-tail features are intrinsic to the quasiparticles and do not arise from some extrinsic sources such as barrier effects or junction heating. Furthermore, the similarity with ARPES (Ref. 34) suggests that a quantitative comparison of the two spectroscopies is important. Neither the smeared BCS DOS nor the *d*-wave DOS gives a good agreement with the data for $eV > 2\Delta$. In particular, we have never observed the sharp decrease in conductance for SIS junctions at $eV = 2\Delta$, which is predicted by BCS *d*-wave theory. What is likely needed to explain all the spectral fea-

tures for $eV>2\Delta$ is a full microscopic theory of the quasiparticle self-energy, analogous to Eliashberg theory for conventional superconductors. We note, for example, that it has been proposed recently that the dip in quasiparticle tunneling is a consequence of electrons interacting with spin excitations, in particular, the sharp resonance mode observed in neutron scattering.[41] If so, then our experiment is indicating that such a resonance feature must persist well into the overdoped region.

Josephson currents are observed as a robust feature of the SIS junctions when the junction conductance exceeds a minimum value of about 10 μS. The maximum critical current I_c scales with junction resistance in a manner consistent with AB theory for *s*-wave superconductors, but with a value of the I_cR_n product that is reduced from that expected using AB theory and the measured quasiparticle gap. Nevertheless, the average value of I_cR_n (2.4 mV) and the maximum value (7 mV) are much larger than expected for the Josephson current between two *d*-wave superconductors assuming incoherent tunneling between the electrodes as is done in AB theory. Therefore, coherent tunneling processes must be important. Since the SIS break junctions studied here are quite similar to the intrinsic, *c*-axis junctions in single crystals, this implies that superconductivity along the *c* direction can be understood in terms of coherent tunneling between Cu-O planes. The increased coherence may be linked to the observed increase in tunneling directionality[38] that is necessary to fit the SIS quasiparticle data. If SIS *c*-axis junctions are dominated by those electrons near $(\pi,0)$ directions, then a more coherent process is immediately obtained.

ACKNOWLEDGMENTS

This work was partially supported by the U.S. Department of Energy, Division of Basic Energy Sciences-Material Sciences, under Contract No. W-31-109-ENG-38, and the National Science Foundation, Office of Science and Technology Centers, under Contract No. DMR 91-20000.

[1] N. Miyakawa, J. F. Zasadzinski, L. Ozyuzer, P. Guptasarma, D. G. Hinks, C. Kendziora, and K. E. Gray, Phys. Rev. Lett. **83**, 1018 (1999).

[2] Y. DeWilde, N. Miyakawa, P. Guptasarma, M. Iavarone, L. Ozyuzer, J. F. Zasadzinski, P. Romano, D. G. Hinks, C. Kendziora, G. W. Crabtree, and K. E. Gray, Phys. Rev. Lett. **80**, 153 (1998).

[3] Z.-X. Shen, D. S. Dessau, B. O. Wells, D. M. King, W. E. Spicer, A. J. Arko, D. Marshall, L. W. Lombardo, A. Kapitulnik, P. Dickinson, S. Doniach, J. DiCarlo, A. G. Loeser, and C. H. Park, Phys. Rev. Lett. **70**, 1553 (1993).

[4] H. Ding, J. C. Campuzano, K. Gofron, C. Gu, R. Liu, B. W. Veal, and G. Jennings, Phys. Rev. B **50**, 1333 (1994).

[5] J. R. Kirtley, C. C. Tsuei, J. Z. Sun, C. C. Chi, L. S. Yu-Jahnes, A. Gupta, M. Rupp, and M. B. Ketchen, Nature (London) **373**, 225 (1995).

[6] C. C. Tsuei, J. R. Kirtley, Z. F. Ren, J. H. Wang, H. Raffy, and Z. Z. Li, Nature (London) **387**, 481 (1997).

[7] C. Kendziora, R. J. Kelley, and M. Onellion, Phys. Rev. Lett. **77**, 727 (1996).

[8] R. J. Kelley, C. Quitmann, M. Onellion, H. Berger, P. Almeras, and G. Margaritondo, Science **271**, 1255 (1996).

[9] Ch. Renner, B. Revaz, J.-Y. Genoud, K. Kadowaki, and O. Fisher, Phys. Rev. Lett. **80**, 149 (1998).

[10] H. Hancotte, R. Deltour, D. N. Davydov, A. G. M. Jansen, and P. Wyder, Phys. Rev. B **55**, R3410 (1997); T. Hasegawa, M. Nantoh, and K. Kitazawa, Jpn. J. Appl. Phys., Part 2 **30**, L276 (1991).

[11] C. Kendziora, R. J. Kelley, E. Skelton, and M. Onellion, Physica C **257**, 74 (1996).

[12] T. Hasegawa, H. Ikuta, and K. Kitazawa, in *Physical Properties of High Temperature Superconductors III* edited by D. M. Ginsberg (World Scientific, Singapore, 1992).

[13] E. L. Wolf, *Principles of Electron Tunneling Spectroscopy* (Oxford University Press, New York, 1985).

[14] Q. Huang, J. F. Zasadzinski, and K. E. Gray, Phys. Rev. B **42**, 7953 (1990).

[15] Ch. Renner and O. Fisher, Phys. Rev. B **51**, 9208 (1995).

[16] Ch. Renner, B. Revaz, J.-Y. Genoud, and O. Fisher, J. Low Temp. Phys. **105**, 1083 (1996).

[17] R. Aoki and H. Murakami, in *Studies of High T_C Superconductors*, edited by A. Narlikar (Nova Scientific, Commack, NY, 1996).

[18] H. J. Tao, A. Chang, F. Lu, and E. L. Wolf, Phys. Rev. B **45**, 10 622 (1992).

[19] D. Mandrus, J. Hartge, C. Kendziora, L. Mihaly, and L. Forro, Europhys. Lett. **22**, 199 (1993).

[20] H. J. Tao, Farun Lu, G. Zhang, and E. L. Wolf, Physica C **224**, 117 (1994).

[21] Q. Huang, J. F. Zasadzinski, K. E. Gray, J. Z. Liu, and H. Claus, Phys. Rev. B **40**, 9366 (1989).

[22] M. Oda, K. Hoya, R. Kubota, C. Manabe, N. Momono, T. Nakano, and M. Ido, Physica C **281**, 135 (1997).

[23] M. E. Hawley, K. E. Gray, B. D. Terris, H. H. Wang, K. D. Carlson, and J. M. Williams, Phys. Rev. Lett. **57**, 629 (1986); L. Ozyuzer, J. F. Zasadzinski, and K. E. Gray, Cryogenics **38**, 911 (1998).

[24] A. Yurgens, D. Winkler, T. Claeson, S. Hwang, and J. Choy, Int. J. Mod. Phys. B (to be published).

[25] H. Won and K. Maki, Phys. Rev. B **49**, 1397 (1994).

[26] R. C. Dynes, V. Narayanamurti, and J. P. Garno, Phys. Rev. Lett. **41**, 1509 (1978).

[27] S. Kashiwaya, Y. Tanaka, M. Koyanagi, and K. Kajimura, Phys. Rev. B **53**, 2667 (1996).

[28] G. E. Blonder, M. Tinkham, and T. M. Klapwijk, Phys. Rev. B **25**, 4515 (1982).

[29] M. Covington, M. Aprili, E. Paraoanu, L. H. Greene, F. Xu, J. Zhu, and C. A. Mirkin, Phys. Rev. Lett. **79**, 277 (1997).

[30] N. Tsuda, K. Nasu, A. Yanase, and K. Siratori, *Electronic Conduction in Oxides* (Springer, New York, 1991).

[31] Z. Yusof, J. F. Zasadzinski, L. Coffey, and N. Miyakawa, Phys. Rev. B **58**, 514 (1998).

[32] P. J. White, Z.-X. Shen, C. Khim, J. M. Harris, A. G. Loeser, P. Fournier, and A. Kapitulnik, Phys. Rev. B **54**, R15 669 (1996).

[33] P. Romano, J. Chen, and J. F. Zasadzinski, Physica C **295**, 15 (1998).

[34] M. R. Norman, H. Ding, J. C. Campuzano, T. Takeuchi, M. Randeria, T. Yokoya, T. Takahashi, T. Mochiku, and K. Kadowaki, Phys. Rev. Lett. **79**, 3506 (1997); Z. X. Shen, P. J. White, D. L. Feng, C. Kim, G. D. Gu, H. Ikeda, R. Yoshizaki, and N. Koshizuka, Science **280**, 259 (1998).
[35] P. Mallet, D. Roditchev, W. Sacks, D. Defourneau, and J. Klein, Phys. Rev. B **54**, 13 324 (1996).
[36] C. Manabe, M. Oda, and M. Ido, J. Phys. Soc. Jpn. **66**, 1776 (1997).
[37] V. Ambegaokar and A. Baratoff, Phys. Rev. Lett. **10**, 486 (1963).
[38] Yung-mau Nie and L. Coffey, Phys. Rev. B **57**, 3116 (1998).
[39] R. A. Klemm, G. Arnold, C. T. Rieck, and K. Scharnberg, Phys. Rev. B **58**, 14 203 (1998).
[40] Y. I. Latyshev, T. Yamashita, L. N. Bulaevskii, M. J. Graf, A. V. Balatsky, and M. P. Maley, Phys. Rev. Lett. **82**, 5345 (1999).
[41] J. P. Carbotte, E. Schachinger, and D. N. Basov, Nature (London) **401**, 354 (1999).